

P. Maget¹, J. Frank^{1,2}, P. Manas¹, R. Dumont¹, T. Nicolas³, J-F. Artaud¹, C. Bourdelle¹, L. Colas¹, M. Goniche¹, O. Agullo², X. Garbet¹, H. Lütjens³ and the WEST team[#]

¹CEA, IRFM, F-13108 Saint Paul-lez-Durance, France.

²Aix-Marseille Université, CNRS, PIIM UMR 7345, 13397 Marseille Cedex 20, France.

³Centre de Physique Théorique, Ecole Polytechnique, CNRS, 91128 Palaiseau, France.

[#] see <http://west.cea.fr/WESTteam>



West

Summary

- Heavy impurity transport is a key issue in metallic wall tokamaks
 - Collisional part can be dominant over turbulent one in the core [1]
- Derivation of a fast analytical model for collisional impurity transport
 - Self-consistent Poloidal asymmetry and radial flux
 - Applicable to rotating & ICR Heated plasmas [2]
 - Compared with XTOR [3,4] simulations, and with NEO [5]
- Investigation on a rare case of Tungsten accumulation on WEST
 - ICRH-driven asymmetry could be the main mechanism

Analytical approach for collisional impurity transport

Neoclassical impurity transport

- With a poloidal distribution parametrized as $n_a/\langle n_a \rangle = 1 + \delta \cos \theta + \Delta \sin \theta$ [1]:

$$\langle \Gamma_a^{neo} \cdot \nabla r \rangle \approx -\langle n_a \rangle \frac{D_{PS}^a}{R_0} \left[\left(1 + \frac{\delta}{\epsilon} + \frac{\delta^2 + \Delta^2}{4\epsilon^2} \right) \mathcal{G} + \frac{1}{2} \left(\frac{\delta}{\epsilon} + \frac{\delta^2 + \Delta^2}{2\epsilon^2} \right) \mathcal{U} - \frac{\delta_M}{2\epsilon^2} \left(1 - \frac{m_i e_a}{m_a e_i} \right) \left(1 + \frac{\delta}{2\epsilon} \right) \right]$$

- with $D_{PS}^a \equiv 2q^* m_a \nu_a T_a / (e_a^2 \langle B^2 \rangle)$, $\epsilon = r/R_0$, $C_0^a \sim 1.5$ and $k_T \sim 1.17$ in the banana regime

$$G = \partial_r \ln p_a - \frac{e_a T_i}{e_i T_a} \partial_r \ln p_i + C_0^a \frac{e_a T_i}{e_i T_a} \partial_r \ln T_i \quad U \approx - (C_0^a + k_i) \frac{e_a T_i}{e_i T_a} \partial_r \ln T_i$$

$$\delta_M = 2\epsilon (m_a/m_i) (T_i/T_a) M_i^2$$

Poloidal asymmetry

- The poloidal asymmetry is given by the parallel force balance

$$\delta + \delta_\phi^a - \delta_M = -\mathcal{A} [\Delta \mathcal{G} + \Delta \mathcal{U} - \mathcal{R} \delta_M \epsilon \Delta]$$

$$\Delta + \Delta_\phi^a = \mathcal{A} [(2\epsilon + \delta) \mathcal{G} + \delta \mathcal{U} - 2\mathcal{R} \delta_M]$$

$$\mathcal{A} = q^2 \nu_a / (\epsilon \Omega_a)$$

$$\mathcal{R} = \frac{1}{2\epsilon} \left(1 - \frac{m_i e_a}{m_a e_i} \right)$$

- With the electrostatic potential modelled as $e(\phi - \langle \phi \rangle) / T_e = \delta_\phi \cos \theta + \Delta_\phi \sin \theta$ and $(\delta_\phi^a, \Delta_\phi^a) = Z_a (T_e/T_a) (\delta_\phi, \Delta_\phi)$

Self-consistent collisional impurity transport model

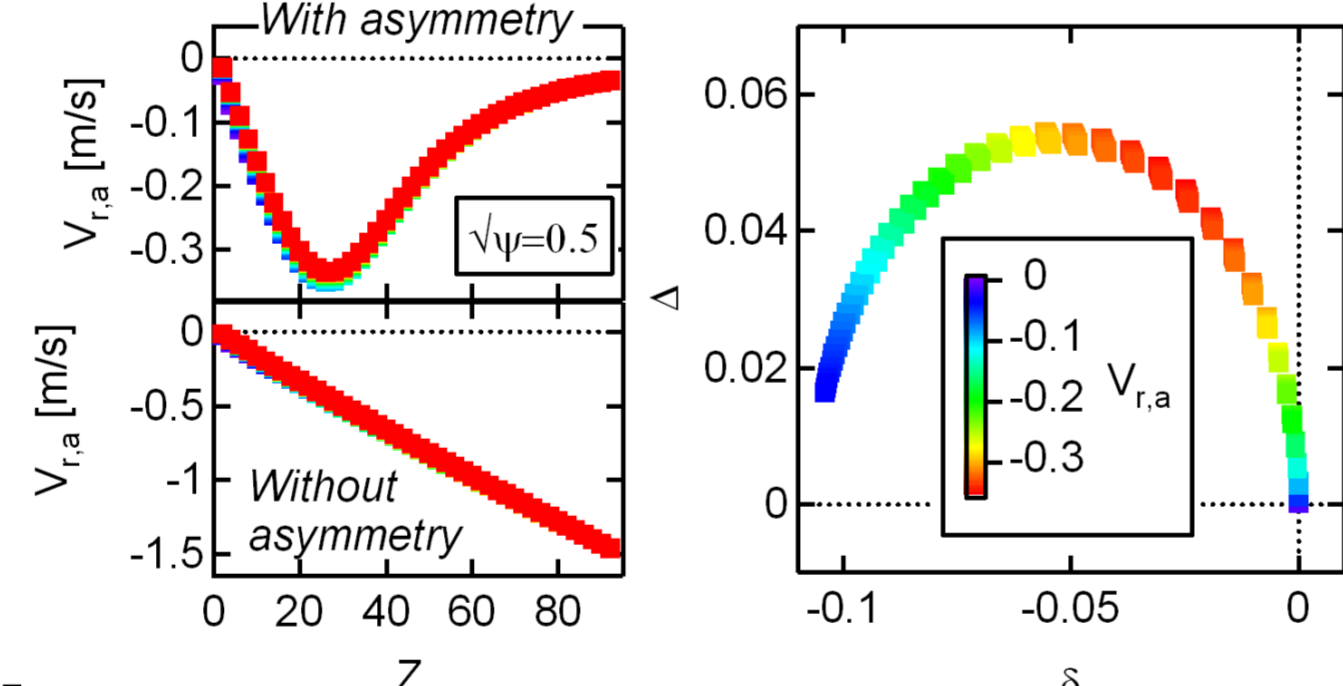
- Implemented in FACIT code (FAst Collisional Impurity Transport)
- Impurity flux & asymmetry are non-linear functions of the impurity gradient
- Collisional friction couples vertical & horizontal asymmetry: tilting w.r.t. the drive

The natural case (no rotation, no ϕ asymmetry)

Poloidal asymmetry parameters (δ, Δ) move on a circle as collisionality varies

- Pinch velocity is strongly reduced by poloidal asymmetry at high Z (flat n_a) [6] (fig.1)

Fig.1 : Radial impurity flow as a function of the impurity charge Z_a with & without self-consistent poloidal asymmetry (left); corresponding asymmetry (right). The impurity profile is flat.



Numerical experiments with XTOR-2F code [2]

- Neoclassical physics [4]
- Impurity conservation and momentum equations
- The collisionality (ν_a) is scanned artificially
- The circle in the (δ, Δ) plane is recovered ...
- ... as well as the reduction of the pinch velocity (fig. 2)

Neoclassical steady-state ($\Gamma^{neo}=0$)

- Poloidal asymmetry cancels (fig. 3)
- XTOR simulation follow same initial trajectory in (δ, Δ)

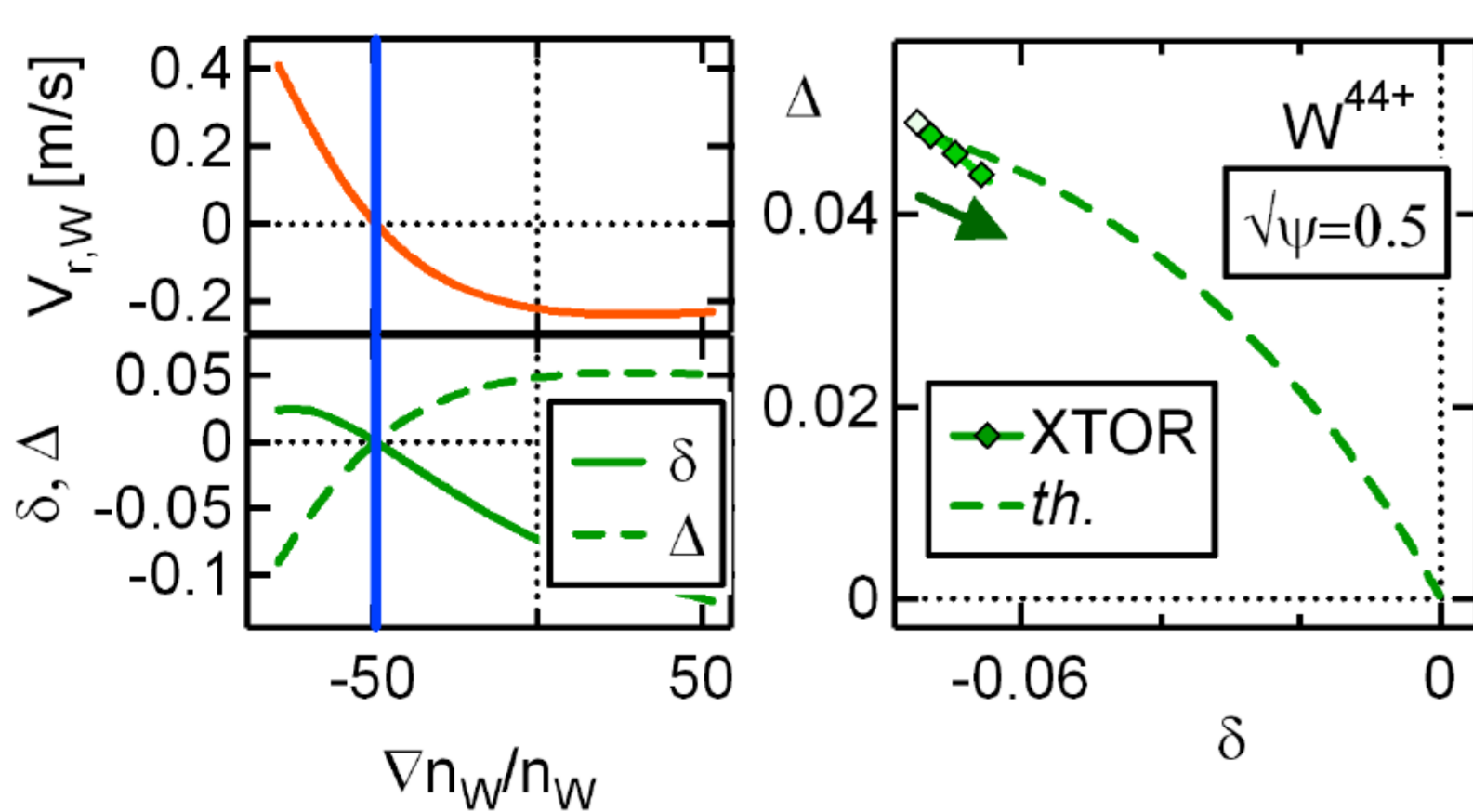


Fig.3 : Left: radial flux (top) and asymmetry (bottom). Right: XTOR simulations & FACIT model

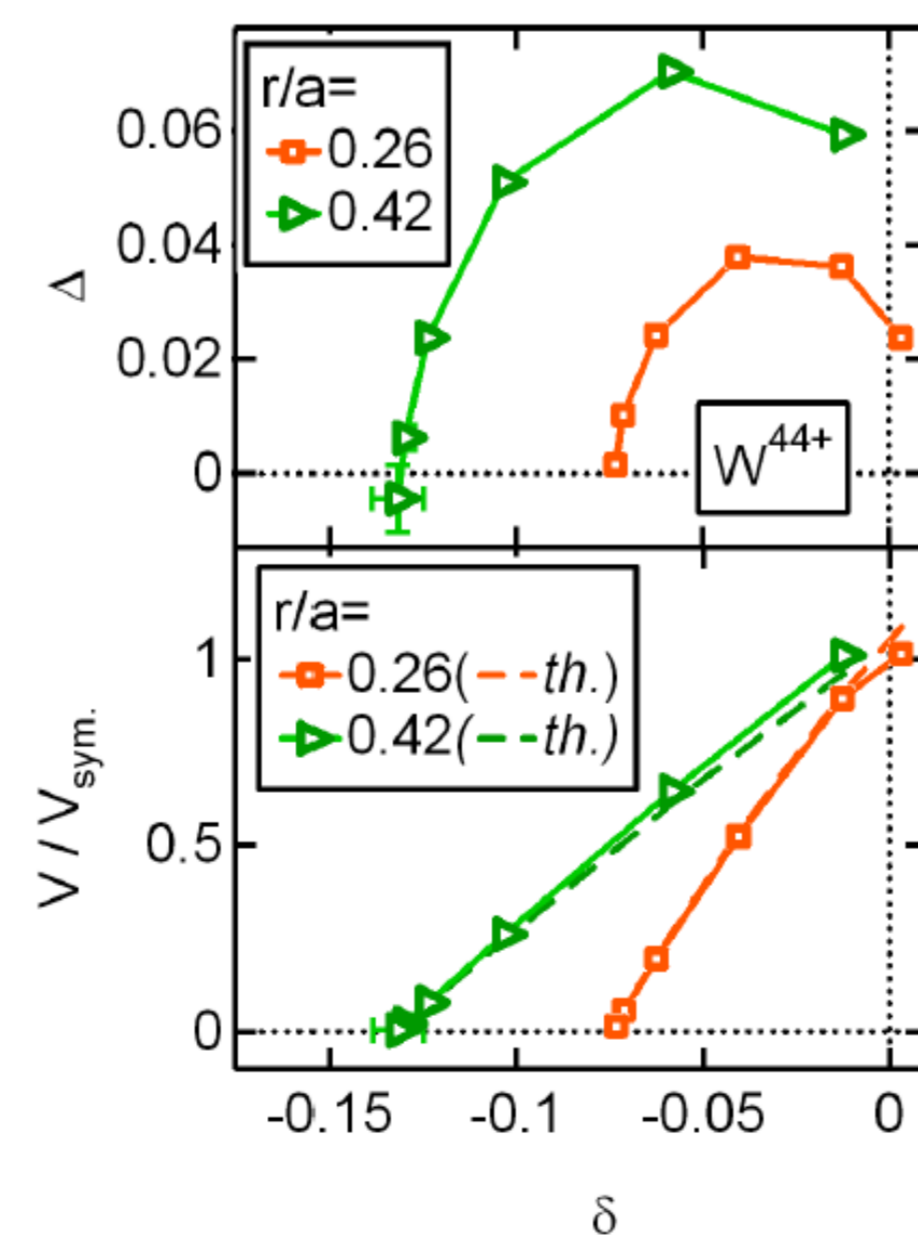


Fig.2 : Asymmetry (top) and ratio of radial flow to theoretical value without asymmetry (bottom): XTOR simulations & FACIT model

References

- [1] Angioni et al *PPCF* **56** 124001 (2014)
 [2] Maget et al, *PPCF* **62** 105001 (2020)
 [3] Lütjens *J. Comp. Phys.* **229** 8130 (2010)
 [4] Maget et al, *PPCF* **62** 025001 (2020)
 [5] Belli et al *PPCF* **50** 095010 (2008)
 [6] Helander *Physics of Plasmas* **5** 3999 (1998)

- [7] Hinton *The Physics of Fluids* **16** 836 (1973)
 [8] Yang *Nuclear Fusion* **60** 086012 (2020)
 [9] Artaud *Nuclear Fusion* **58** 105001 (2018)
 [10] Dumont *NF* **49** 075033 (2009); *NF* **53** 013002 (2012)

Collisional vertical ϕ - asymmetry effect

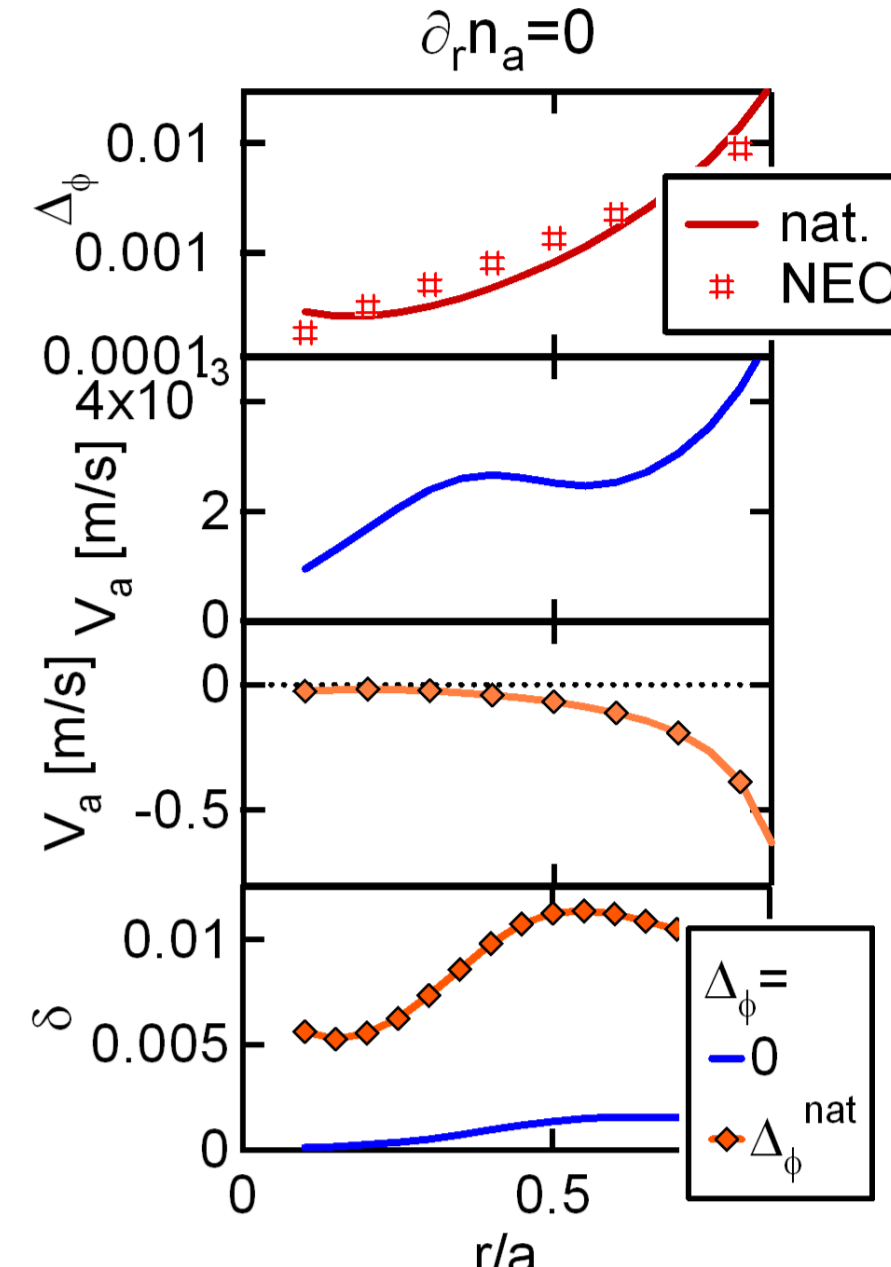
Extension of the natural case to finite ϕ - asymmetry

- Ion-electron collisions drive a vertical ϕ - asymmetry [7]

$$\Delta_\phi^{nat} \approx \frac{C^{nat}}{Z_i + T_e/T_i} \frac{q^2 x \partial_x \ln T_i}{\epsilon^{5/2} \tau_{ii} \Omega_i} \quad \text{with } C^{nat} \approx -0.165$$

- Asymmetry recovered with NEO at 1st order : not used for computing impurity flux
- But in fact, it strongly impact impurity flux & poloidal asymmetry in the absence of other drives (no rotation & no ICRH) (fig.4)
- Only effective at low T_i

Fig.4 : Natural vertical electrostatic potential asymmetry profile, pinch velocity and horizontal asymmetry with and without Δ_ϕ^{nat} .

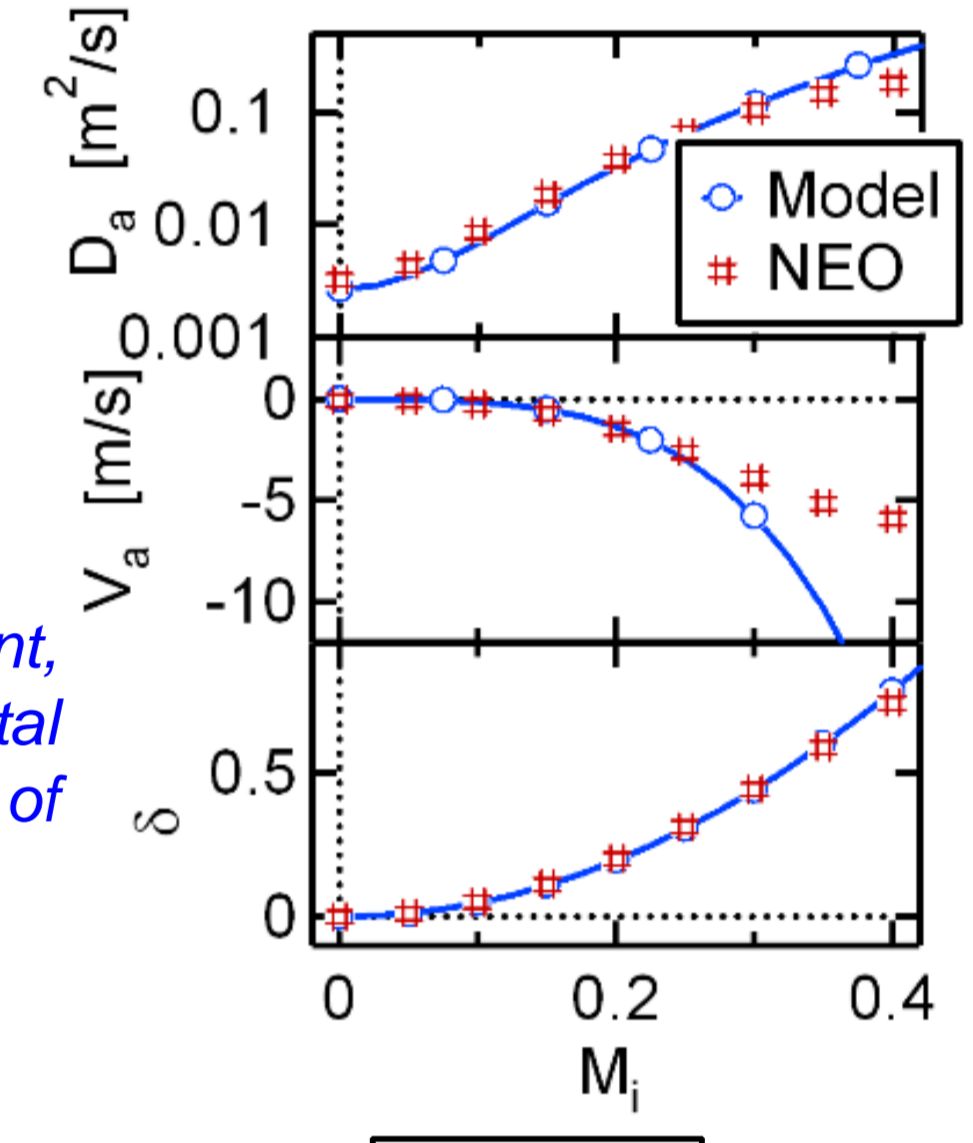


Toroidal rotation and ICRH effect

Toroidal rotation

- Neoclassical diffusion coefficient, pinch velocity and horizontal asymmetry at $\Gamma^{neo}=0$ in good agreement with NEO for $M_i < 0.3$ (fig. 5)
- Pinch velocity overestimated above $M_i < 0.3$
- Low Field Side localization due to centrifugal force

Fig.5 : Diffusion coefficient, pinch velocity and horizontal asymmetry as a function of the ion Mach number.



ICRH

- Minority temperature anisotropy : horizontal ϕ -asymmetry

$$\delta_\phi = \frac{\epsilon}{1 + Z_i T_e/T_i} \left[f_H \left(\frac{T_\perp}{T_\parallel} - 1 \right) + m_i \frac{(R_0 \Omega)^2}{T_i} \right]$$

- Neoclassical diffusion coefficient, pinch velocity and horizontal asymmetry at $\Gamma^{neo}=0$ agrees with NEO (fig.6)
- High Field Side localization due to electrostatic force
- Transition from expulsion to accumulation above a critical temperature anisotropy
- Neoclassical diffusion vanishes at the transition: classical diffusion dominant
- Favorable domain $T_\perp/T_\parallel < (T_\perp/T_\parallel)^{crit}$ expands with M_i as

$$\left[f_H \left(\frac{T_\perp}{T_\parallel} - 1 \right) \right]^{crit} \approx 2 \frac{Z_i + T_e/T_i}{Z_a} + 2 M_i^2 \left[\frac{m_a Z_i + T_e/T_i}{m_i Z_a} - 1 \right]$$

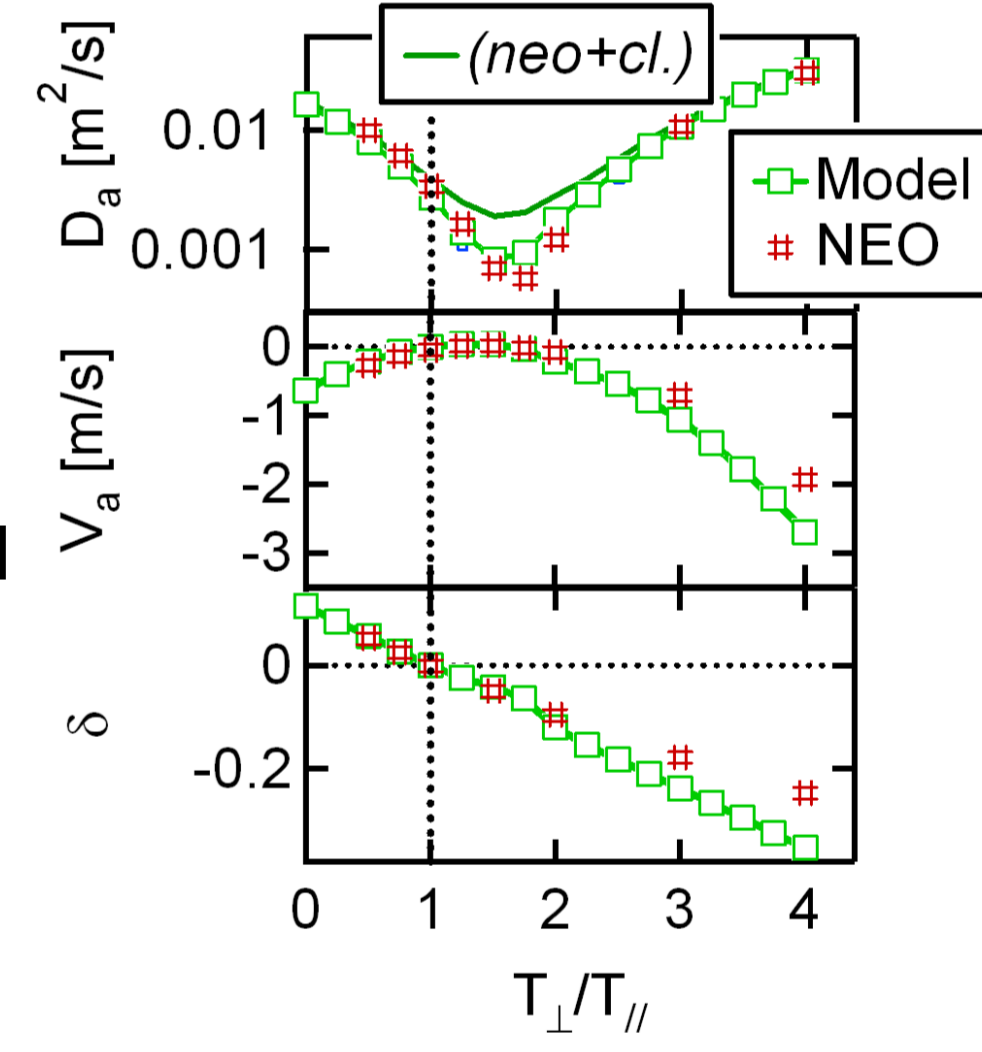


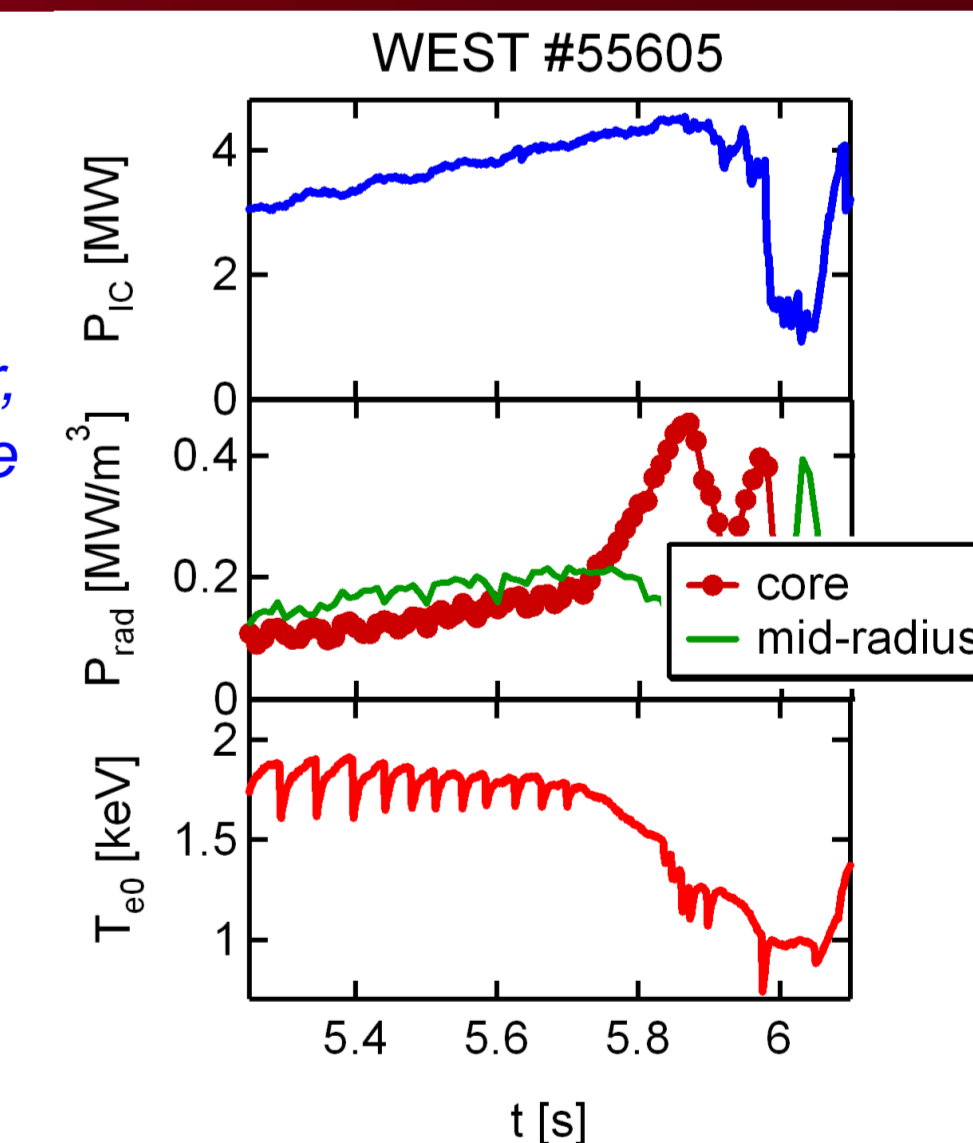
Fig.6 : Diffusion coefficient, pinch velocity and horizontal asymmetry as a function of T_\perp/T_\parallel .

Tungsten peaking & ICRH operation: a WEST case

Rare cases of Tungsten accumulation on WEST

- Low torque plasma: turbulent transport dominates [8]
- Accumulation observed in some ICRH pulses (fig.7)

Fig.7 : ICRH power, radiative power and core electron temperature.



Modeling of Tungsten peaking

- Interpretative Integrated modeling with METIS [9]
- Ion temperature deduced neutron flux & $T_i \propto \sqrt{n_e T_e}$
- Minority temperature anisotropy : EVE/AQL [10] (fig. 8)
- Minority temperature screening effect not considered
- Toroidal rotation not measured but (4,1) MHD mode accelerates linearly with ICRH power (fig.9)
- Rotation: $V_\phi = V_0 + (V/P) \times P_{IC}$ with $(V/P) \sim 3 \text{ km/s/MW}$
- Tungsten peaking from FACIT consistent with ICRH drive at low rotation ($V_\phi \sim 0$) (fig.10)

WEST #55605 - Mirnov coil

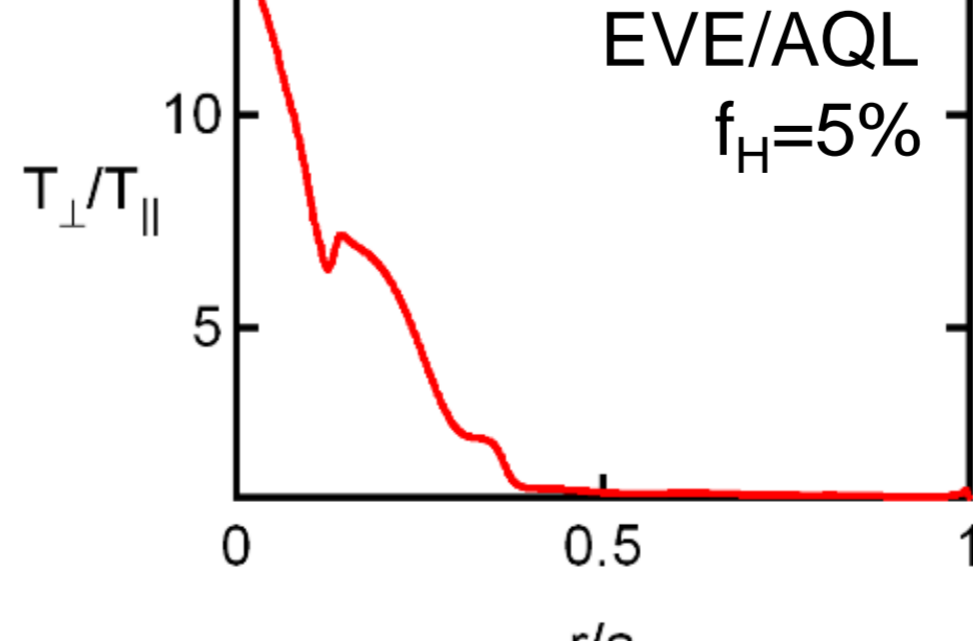


Fig.8 : H temperature anisotropy from EVE/AQL

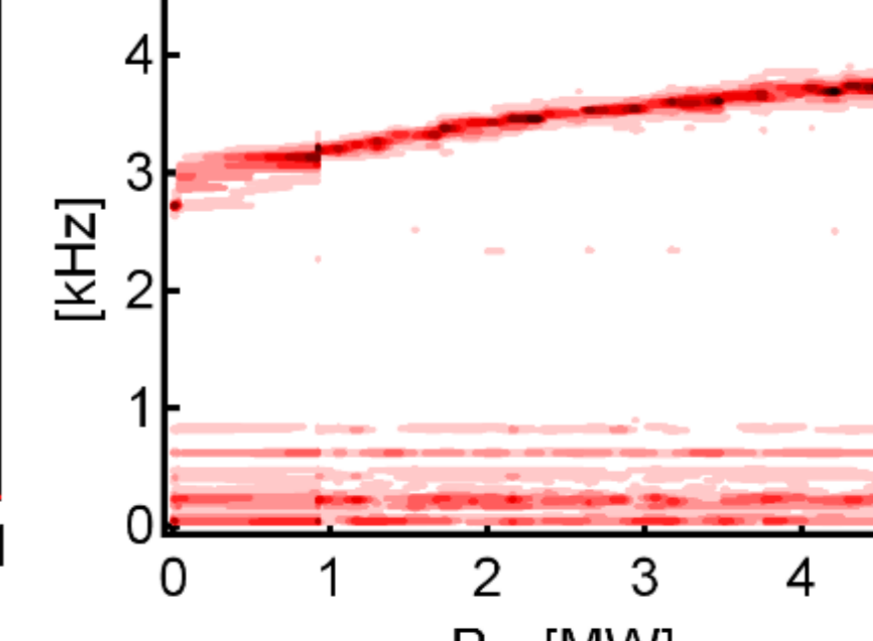


Fig.9 : MHD mode rotation as a function of P_{IC} .

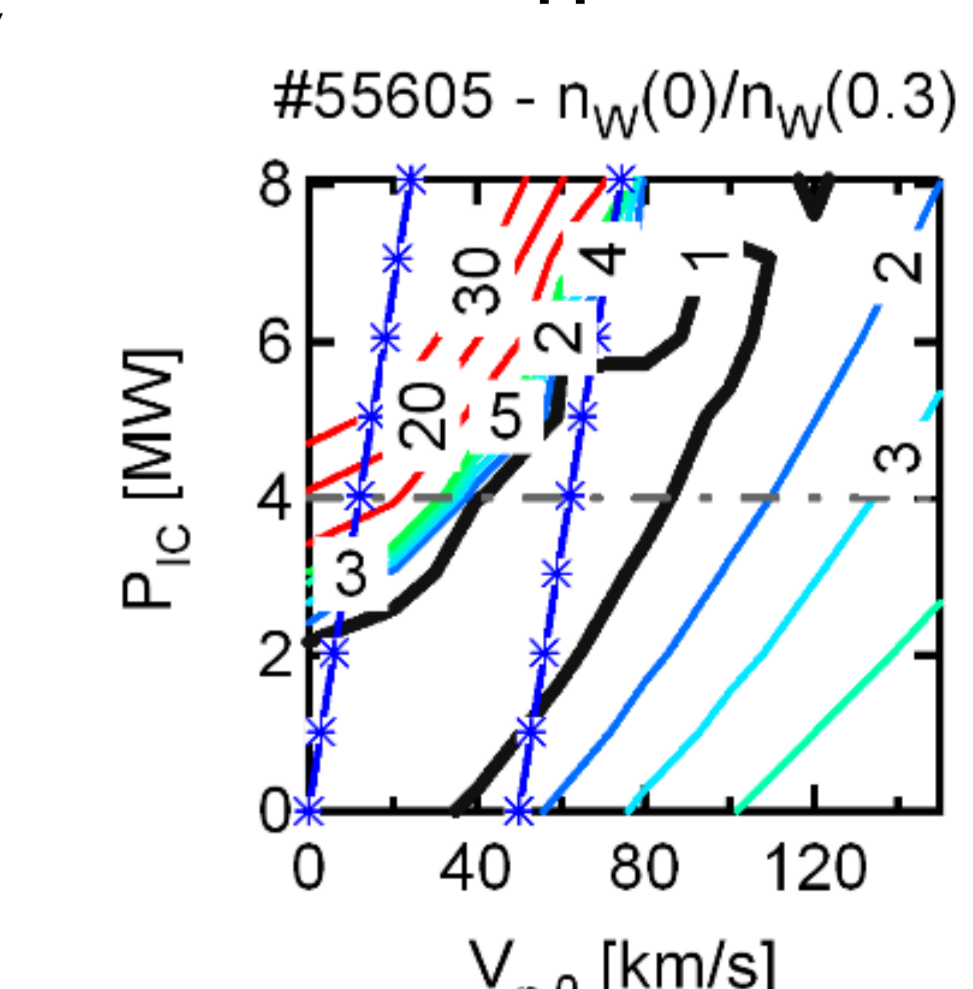


Fig.10 : Tungsten peaking in (P_{IC}, V_ϕ) map. Trajectories for $V_\phi = 0$ and 50 km/s

Acknowledgements

This work has been carried out within the framework of the EUROfusion Consortium and the French Research Federation for Fusion Studies and has received funding from the Euratom research and training programme 2014-2018 and 2019-2020 under grant agreement No 633053 for the project ENR-MFE19.CEA-03. We benefited from HPC resources from GENCI (project 056348). The views and opinions expressed herein do not necessarily reflect those of the European Commission.